High pressure growth of bulk GaN from solutions in gallium

2001 J. Phys.: Condens. Matter 13 6875

(http://iopscience.iop.org/0953-8984/13/32/301)

INSTITUTE OF PHYSICS PUBLISHING JOURNAL OF PHYSICS: CONDENSED MATTER

J. Phys.: Condens. Matter **13** (2001) 6875–6892 PII: S0953-8984(01)24776-6

High pressure growth of bulk GaN from solutions in gallium

Izabella Grzegory

High Pressure Research Center, Polish Academy of Sciences, ul. Sokołowska 29/37,
01-142 Warsaw, Poland

E-mail: izabella@unipress.waw.pl

Received 11 May 2001
Published 26 July 2001
Online at stacks.iop.org/JPhysCM/13/6875

Abstract

In this paper, the growth of GaN single crystals from solutions of atomic nitrogen in liquid gallium under high N_2 pressure is described. GaN single crystals obtained by the high nitrogen pressure solution method, without an intentional seeding, show strong growth anisotropy, which results in their platelet shape. The attempts to enhance the growth into (0001) directions by the increase of the integral supercooling in the solution often lead to growth instabilities on both N-polar and Ga-polar (0001) surfaces. This can be avoided only by the precise control of the growth conditions at the crystallization front on the particular surface.

The results of the seeded growth in directions parallel and perpendicular to the *c*-axis of GaN are discussed. In particular, it is shown that dominating mechanisms of the unstable growth on (0001) polar surfaces such as the cellular growth or edge nucleation can be suppressed and the crystal can be grown in a much more stable way.

Physical properties most relevant for understanding the growth of GaN crystals are reviewed. The most important feature of GaN crystals grown by the HNPS method is that they are almost free of dislocations and therefore used as substrates give a possibility to grow perfect epitaxial structures.

1. Introduction

It would be fantastic to have big, dislocation free GaN crystals as is possible for other III–V semiconductors: GaAs, GaP, InP. Even without them, the physical properties of GaN based layer structures are fascinating and of huge practical importance [1]. This is first of all due to the great achievements in GaN technology allowing lower dislocation densities in the material grown on mismatched sapphire and SiC substrates [1] and allowing us to obtain p-type GaN and AlGaN [2]. This is also due to the unusual properties of InGaN, in which at low

0953-8984/01/326875+18$30.00

excitations, the radiatively recombining excitons localized in potential minima are not affected by dislocations, which are the centres for non-radiative recombination [3]. So the III–N based quantum structures containing InGaN, are much more 'tolerant' to the crystal lattice defects than the structures based on typical III–V compounds like GaAs. But also for InGaN-based structures, especially for high excitation applications, the best solution is to eliminate defects by the use of lattice-matched substrates for epitaxial growth. There are several technological approaches to lower dislocation densities in GaN-based materials like the use of the epitaxial lateral over-growth technique for substrates [4], the use of multiple low temperature buffer layers [5] and obviously the attempts to grow bulk GaN [6–8] and AlN [9] dislocation free crystals.

In this paper, we show what the fundamental reasons are for difficulties in the growth of bulk GaN and what can be done anyway even in the simplest system containing GaN, i.e. the nitride with its elemental constituents.

2. Thermodynamical properties of GaN–Ga–N_2 system

Table 1 compares melting temperatures and pressures of most typical semiconductor materials. The melting temperature T^M, and the corresponding equilibrium pressure at melting, of GaN as for other III–N compounds has not been measured. The melting temperature has been calculated by the use of Van Vechten's quantum dielectric theory of chemical bonding [10]. The corresponding pressure follows from the extrapolation of the experimental equilibrium data [11, 12]. The table shows that both temperature and pressure at melting of GaN are much higher that for typical semiconductors. They are rather similar to the conditions used for high pressure synthesis of diamond.

Table 1. Melting conditions of semiconductors.

Crystal	T^M (°C)	p^M (atm.)
Si	1400	<1
GaAs	1250	15
GaP	1465	30
GaN	**2500**	**45 000**
Diamond (synthesis)	1600	60 000

Due to these extreme melting conditions, GaN (like AlN and InN) cannot be grown from its stoichiometric melt by the Czochralski or Bridgman methods commonly used for typical semiconductors. It has to be crystallized by methods allowing lower temperatures and pressures.

Gallium nitride is a strongly bonded compound (with bonding energy of 9.12 eV/atom pair [13]) in comparison with typical III–V semiconductors like GaAs (bonding energy of 6.5 eV/atom pair). Consequently, the free energy of the crystal is very low in relation to the reference state of free N and Ga atoms. On the other hand, the N_2 molecule is also strongly bonded (4.9 eV/atom). Therefore, the free energy of GaN constituents at their normal states, Ga and N_2, becomes quite close to that of the crystal. This is illustrated in figure 1, where the free energy of GaN (1 mole) and the free energy of the system of its constituents (Ga + $\frac{1}{2}N_2$) is shown as a function of temperature and N_2 pressure. With increasing temperature, $G(T)$ of the constituents decreases faster than $G(T)$ of the crystal and at higher temperatures, the nitride becomes thermodynamically unstable. The crossing of the $G(T)$ curves determines the

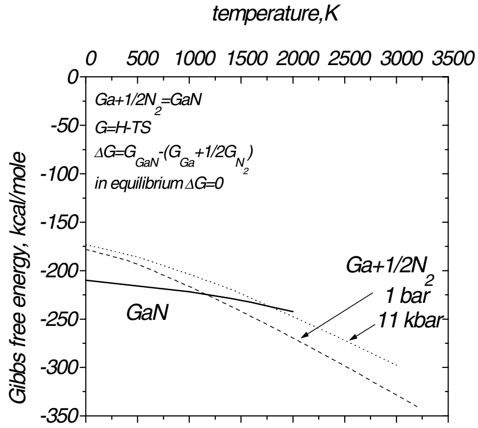

Figure 1. Gibbs free energy of GaN and its constituents.

equilibrium temperature where GaN coexists with its constituents at given N_2 pressure. The application of pressure increases the free energy of the constituents to a much higher degree than $G(T)$ of the crystal. As a consequence the equilibrium point shifts to higher temperatures and the GaN stability range extends. The equilibrium p_{N_2}–T conditions for GaN have been studied by several groups [11, 14–16]. The most complete and consistent results have been obtained by Karpinski *et al* [11, 12] by direct synthesis and decomposition experiments performed by both the gas pressure technique (for pressures up to 20 kbar) and the high pressure anvil technique (up to 70 kbar). The curve following from these data is shown in figure 2. The crystallization processes discussed in this paper have been carried out at N_2 pressure up to 20 kbar, which corresponds to the GaN stability limit of 1960 K. These conditions are marked in figure 2. As shown in [12] for pressures up to 20 kbar, the equilibrium curve can be described by the van't Hoff equation:

$$\Delta H_F = \frac{1}{2} R \frac{\mathrm{d} \ln a_{N_2}}{\mathrm{d}(1/T)} \tag{1}$$

where ΔH_F is the formation enthalpy of GaN, a_{N_2} is the equilibrium activity of N_2 gas, with ΔH_F constant and equal to -37.7 kcal mol^{-1}.

The extension of the GaN stability range by the application of pressure allows us to grow GaN crystals from the solution in the liquid Ga. In figure 3 we have shown the experimental N solubility data [13] resulting from the annealing of Ga in N_2 atmosphere at the three phase equilibrium conditions. Even the highest available temperature of 1960 K is quite far from the melting temperature of GaN (table 1). Therefore the N concentrations are not high (below 1 at.%) and the growth experiments have to be long to get high quality crystals with dimensions appropriate for research and applications. Therefore the long time (>100 h) of stable work is an additional requirement for the growth system. The solid line in figure 3 is the liquidus line for the Ga–GaN system calculated in the ideal solution approximation with Van Vechten's melting temperature of 2790 K. For this approximation the solubility can be expressed as follows:

$$n = n_0 \exp \frac{\Delta H_{sol}}{kT} \tag{2}$$

where ΔH_{sol} is the heat of dissolution. For GaN, $\Delta H_{sol} = 44.7$ kcal/mole $= 0.49$ eV/bond and expresses the bonding energy in the crystal in relation to its mother phase—the solution [13].

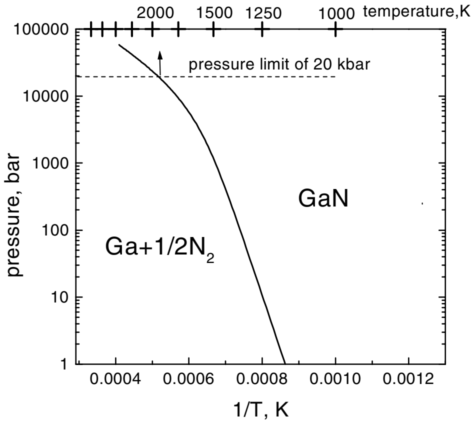

Figure 2. Equilibrium curve for GaN [11, 12].

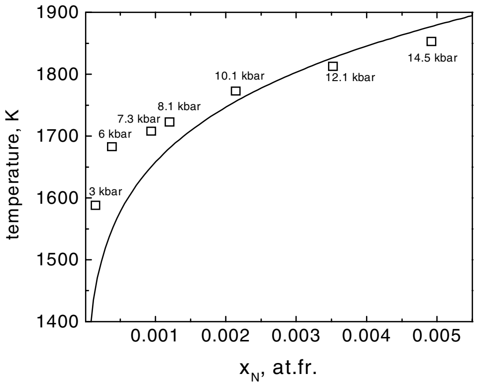

Figure 3. Liquidus line for Ga–GaN system: the solid line was calculated in the ideal solution approximation.

The analysis of thermodynamical properties of the system of GaN and its constituents explains the role of high pressure as a factor increasing the thermodynamical potential of the constituents, which makes the crystal stable at temperatures necessary for crystallization. The pressure however is important also for kinetics of GaN synthesis. The synthesis of GaN from its constituents is possible due to dissociative chemisorption of the N_2 molecule on the Ga surface as shown by Krukowski *et al* by density functional theory calculations [17]. The nitrogen molecule dissociates on the Ga surface only if it overcomes the potential barrier of about 3.5 eV. Therefore as shown in [17] the density of the interacting gas is of crucial importance for the Ga–N_2 system. So, the molecular nitrogen in contact with gallium dissociates at the surface and dissolves in the metal in the atomic form. If the N_2 pressure exceeds the equilibrium one for the GaN–Ga–N_2 system, the formation of a GaN crystalline crust on the metal surface is observed [13, 18]. The structure of this crust depends on the overpressure applied and on the method of creation of the synthesis conditions [13]. For small overpressures, the size of the crystals creating the crust can be as big as shown in figure 4.

At isothermal conditions, further synthesis of GaN is hindered once the whole gallium surface covers with the crust. Hence the transport of nitrogen in the metal has to be enforced

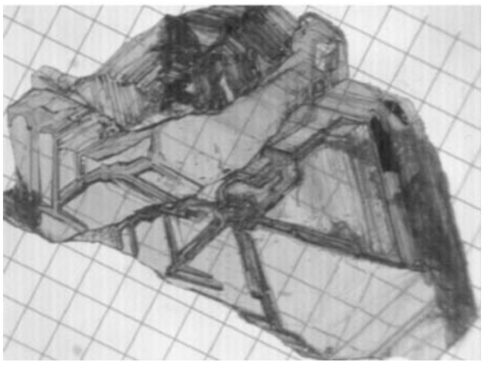

Figure 4. GaN crystal grown on the Ga surface at 1500 °C, at about 100 bar N_2 overpressure. The distance between grid lines is 1 mm.

Figure 5. The result of GaN synthesis from the liquid Ga and N_2 plasma. The liquid has been pushed out from the initial droplet covered by GaN crust, by the growing N_2 bubbles.

to continue crystallization of GaN from the solution. Both the increase of thermodynamical potential of gaseous nitrogen and the enhancement of the creation of the atomic nitrogen at the Ga surface can be achieved by other (not compression) methods like the excitement of N_2 plasma or the use of species containing nitrogen atoms bonded weaker than in N_2 molecule. It was demonstrated [18, 19] that in microwave nitrogen plasma of 60 Torr and temperature as low as 1100 °C, a very efficient GaN (and even InN!) synthesis is possible. The excited N_2 gas was very efficient source to saturate a Ga droplet with atomic nitrogen and to form GaN crust on the droplet surface. However since the pressure in the system was much lower than the equilibrium one (about 100 bar for 1100 °C), the N_2 gas phase started to nucleate and grow in the liquid. This resulted in the formation of the structure shown in figure 5, which was the empty ‘Ga droplet’ covered with irregular polycrystalline GaN.

The formation of the N_2 bubbles in the supersaturated Ga:N liquid was also observed if the pressure in the system containing GaN crystals dipped in the Ga:N solution was intentionally decreased below the equilibrium value. Then the N_2 bubbles nucleated on the surface of the crystals and the crystals locally in contact with the gas started to decompose trying to restore

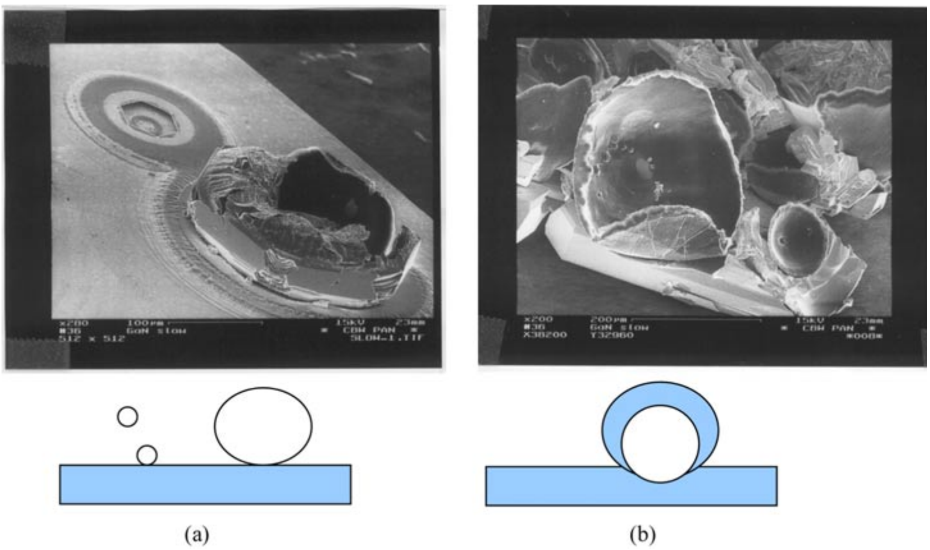

Figure 6. Decomposition of GaN in the supersaturated Ga:N solution if the pressure in the system drops below the equilibrium value. Local decomposition features supporting the proposed mechanism are visible on the crystal surfaces. (a) N_2 bubbles start to nucleate in the liquid, some of them nucleate on the GaN crystal surfaces; (b) during cooling the interfaces are covered with GaN since the solution is supersaturated.

the equilibrium. During cooling of the system, the interface between the gas bubbles and the surrounding liquid covered with GaN crystallized from the supersaturated solution. Two examples of GaN crystals with local decomposition features on their surfaces are shown in figure 6 together with the schematic illustration of the described process.

3. Experiment

At present, GaN is crystallized in gas pressure chambers with volume up to 1500 cm^3 allowing crucibles with the working volume of 50–100 cm^3. The high pressure—high temperature reactor consisting of the pressure chamber and the multizone furnace is equipped with additional systems necessary for *in situ* annealing in vacuum, electronic stabilization and programming of pressure and temperature and cooling of the pressure chamber. Pressure in the chamber is stabilized with precision better than 10 bar. The temperature is measured by a set of thermocouples arranged along the furnace and coupled with the standart input power control electronic systems based on Eurotherm units. This allows stabilization of temperature ±0.2 K and programmable changes of temperature distribution in the crucible.

GaN crystals presented in this paper were grown from the solutions in pure liquid gallium and in Ga alloyed with 0.2–0.5 at.% of Mg or Be at pressures in the range of 10–20 kbar and temperatures of 1400–1600 °C. Magnesium and beryllium as the most efficient acceptors in GaN were added to the growth solutions in order to reduce the concentration of free electrons in the crystals by compensation of residual donors.

The supersaturation in the growth solution has been created by the application of temperature gradient of 2–20 °C cm^{-1} along the axis of the crucible. This method was chosen since the axial temperature gradients in multizone furnaces working at high gas pressure can be controlled with high precision and the method assures a continuous flow of nitrogen from the hotter part of the solution to the cooler one. If the crystallization experiments were performed without an intentional seeding, the crystals nucleated spontaneously on the internal surface of polycrystalline GaN crust covering liquid Ga at the cooler zone of the solution. The typical duration of the processes was 120–150 hours.

The slow cooling at isothermal conditions was not applied due to small concentrations of nitrogen in the liquid gallium (figure 3). The crystallization at constant temperature, at N_2 overpressure was not applied as well since then the crystallization can occur only on the Ga surface and stops if the whole surface is covered with GaN.

4. GaN crystals grown without intentional seeding

The GaN crystals grown by the high nitrogen pressure solution method are of wurzite structure, mainly in the form of hexagonal platelets. The large hexagonal surfaces correspond to {0001} polar crystallographic planes. The side faces of the crystals are mainly the polar $\{10-11\}$ and also non-polar $\{10-10\}$ planes.

The crystals in the form of hexagonal platelets grown slowly, with a rate <0.1 mm h^{-1} into $\{10\underline{1}0\}$ directions (perpendicular to the *c*-axis), are usually single crystals of perfect morphology suggesting stable layer-by-layer growth. They are transparent, with flat-mirror-like faces. In some cases three dimensional, hexagonal growth figures growing during cooling of the system after crystallization in a temperature gradient are observed on the crystal surfaces so polishing is necessary before using the crystals as substrates for epitaxial growth. The habit of the crystals does not change for solutions containing Mg or Be. The average size of crystals grown without an intentional seeding scales with the diameter of the high pressure reactor as shown in figure 7.

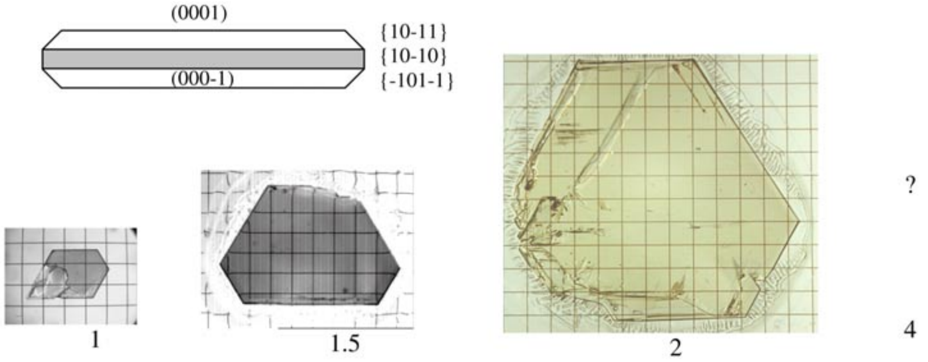

Figure 7. GaN crystals grown at high pressure in chambers of different size. The numbers are proportional to the diameters of the chambers. The distances between grid lines correspond to 1 mm. The schematic cross-section of the hexagonal platelet is shown.

As one can deduce from the form of the crystals the growth is strongly anisotropic being much faster (about 100 times) in directions perpendicular to the *c*-axis. This relation is valid at supersaturations corresponding to the average growth rate in $\{10\underline{1}0\}$ directions of 0.05–0.1 mm h^{-1}.

High supersaturations enhance the growth into the *c*-direction which leads to the unstable needle-like forms. The supersaturation in the growth solution is determined mainly by the growth temperature, temperature gradients, mass transport mechanisms in gallium and also by the local surroundings for a particular crystal (neighbouring crystals). For crystallization of

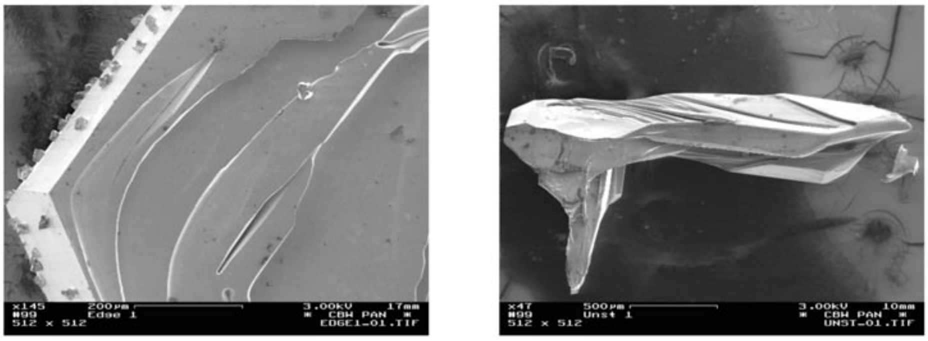

(a)

(b)

Figure 8. (a) Edge nucleation on the (0001) face of a pressure grown GaN crystal. (b) A hollow GaN crystal with the (10$\underline{1}$0) face formed at increased supersaturation.

large GaN crystals, it is crucial to control the supersaturation in order to avoid acceleration of the growth near edges and corners of the growing crystal. If supersaturation is too high, the edge nucleation on hexagonal faces of GaN platelets is often observed, which is the first step to the unstable growth on that faces. The result of such a growth is shown in figure 8(a).

In the extreme cases of very high supersaturations, the growth into the c-direction nucleated at the edges of the plate, becomes very fast, which leads to the formation of well developed $\{10\underline{1}0\}$ faces. Since the lateral growth on the c-face is still slow, the resulting crystals are hollow needles elongated into the c-directions (figure 8(b)).

The tendency for the unstable growth is stronger for one of the polar {0001} faces of the platelets. On this side the morphological features like macrosteps, periodic inclusions of solvent or cellular growth structures are observed. The opposite surface is always mirror-like and often atomically flat. For crystals grown without an intentional doping (strongly n-type—see the next section) the unstable surface always corresponds to the Ga-polar (0001) face of GaN, whereas for crystals doped with Mg (semi-insulating—see the next section) it is always the opposite N-polar (000-1) face. Therefore doping with Mg (if sufficient to compensate free electrons) changes microscopic growth mechanisms on the {0001} polar surfaces of GaN. If the doping level is too low and the resulting crystals are still n type, the morphology is like that for crystallization without doping. This suggest that the position of the Fermi level in the crystal influences the microscopic processes occurring on the growing surfaces. Such a suggestion is consistent with the results of *ab initio* calculations [23, 24] showing that the formation energies of both native and impurity related point defects in GaN are very sensitive to the position of the Fermi level in the crystal.

Figure 9 shows the cross section SEM scan of the n-type GaN platelet. Periodic structure is visible on the Ga-polar (0001) surface of the crystal. Such features are often observed in many of the solution grown crystals as a result of constitutional supercooling of the growth solution at the crystallization front. This will be explained in the next section and the method to suppress such a kind of instability will be discussed.

The polarity of the crystal surfaces was identified by etching in hot alkali water solutions since the Ga-polar surface is inert to etching whereas the N-polar one etches well for both types of crystal. The method was calibrated by CBED [20, 21] and XPS [22] measurements.

From the analysis of the growth of GaN crystals without an intentional seeding it was deduced that the growth into the $\langle 10-10\rangle$ directions, at the conditions corresponding to the

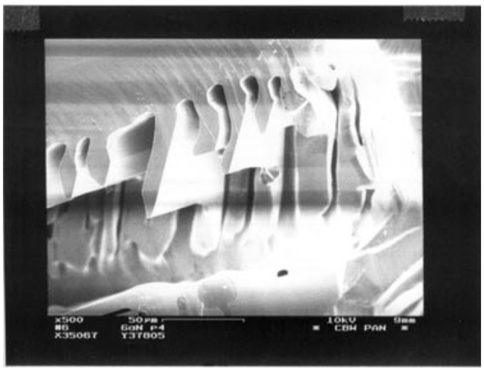

Figure 9. Cellular growth on the Ga-polar (0001) surface of the GaN crystal.

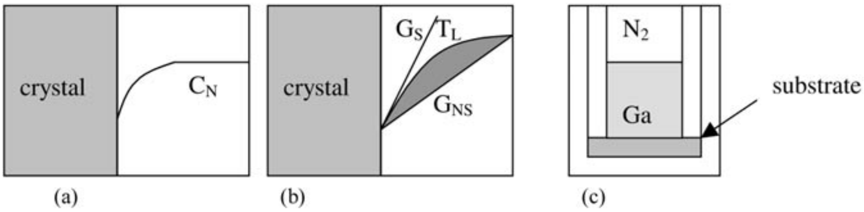

Figure 10. Schematic illustration of constitutional supercooling at the crystallization front: (a) creation of the depleted zone at the crystallization front due to incorporation of the solute into the growing crystal; (b) different temperature gradients applied at the crystallization front related to the equilibrium liquidus temperature profile corresponding to the concentration profile of figure 10(a); (c) configuration used for seeded growth of GaN on {0001} polar surfaces of GaN substrates.

growth rate of 0.05–0.1 mm h^{-1}, is stable and that at the same conditions, the growth into directions $\langle 11-20 \rangle$ (figure 14) is also stable and even faster. Therefore the size of the stable platelets should be a function of the growth time (and volume of the solution) and further scaling of the crystal size with time and the volume of the crucible is possible. It is also clear that the seeded growth into directions perpendicular to the *c*-axis should occur fast and in a stable way, especially into directions $\langle 11-20 \rangle$.

Seeded growth into directions parallel to the *c*-axis seems to be much more challenging since the observed growth rates are small and the growth shows strong tendencies to be unstable. In the next section, the results of seeding are presented.

5. Seeded growth of GaN by HNPS method

The thin GaN platelets described in the previous section can be used for further crystallization as seed crystals. Depending on seed preparation and on the configuration of the experiment it is possible to enforce the growth in directions perpendicular or parallel to the *c*-axis of GaN. As already mentioned, the growth on the {0001} polar surfaces of GaN is very slow and often unstable. Main features of the surface morphology like macrosteps at the edges and the periodic cellular structures suggest possible mechanisms of the unstable growth.

For macrosteps at the edges the quite obvious reason is the accelerated growth at the edges exposed to the nitrogen flux coming from the hot part of the solution. This can be avoided by the elimination of the edges by the proper configuration of the intentional seeding experiment as shown in figure 10(c). Such a configuration allows also to achieve much more uniform supersaturation across the growing surface which is very important condition for stable solution growth especially if the growing surfaces are relatively large.

The cellular growth is often a result of constitutional supercooling [25] of the solution which is graphically explained in figures 10(a) and (b). If the crystallization takes place at the given crystal surface, from the solution of the concentration C_N, a depleted zone at the crystallization front creates due to the incorporation of the solute into the crystal (figure 10(a)). The concentration profile at the growth front can be transformed onto the temperature profile (T_L on figure 10(b)) via the liquidus relation. This temperature profile can be related to the real temperature gradient at the crystallization front. If the gradient is relatively small—like the one labelled G_{NS}, the supersaturation in front of the growing surface can be bigger than at the surface itself. Then, each local acceleration of the growth results in its further enhancement, local depletion at the sides of the growing cell and the formation of a periodic cellular structure like the one shown in figure 9. The condition for stable growth can be expressed by the relation [26]

$$\frac{G_L}{V} > -\frac{C(1-k)(-m)}{kD} \tag{3}$$

where G_L is the temperature gradient at the crystallization front, V is the growth rate, k the distribution coefficient and m the diffusion coefficient of the solute in the growth solution. The parameters on the left-hand side of the relation (3) can be controlled experimentally if the configuration of the experiment corresponds to the scheme of figures 10(a) and (b) or (c).

The n-type GaN platelets have been used for seeded crystallization in order to suppress the cellular growth on the Ga-polar (0001) surface. The N-polar (000-1) surfaces have been also used for comparison. The surfaces were prepared as for epitaxy: they have been polished mechanically and then the subsurface damage has been removed by mechano-chemical polishing for the N-polar surface [27] and by reactive ion etching for the Ga-polar surface.

The experiments were performed in vertical configuration similar to that from figure 10(c). Large positive temperature gradients of the order of 100 °C cm^{-1} have been applied at the average crystallization temperature of about 1500 °C. After 20–50 h processes the substrates with the new crystals deposited on the {0001} surfaces were removed from the solution and investigated. The result of the 50 h growth on the Ga-polar surface is shown in figure 11, where both the optical and SEM images of the substrate with the new grown crystal are presented.

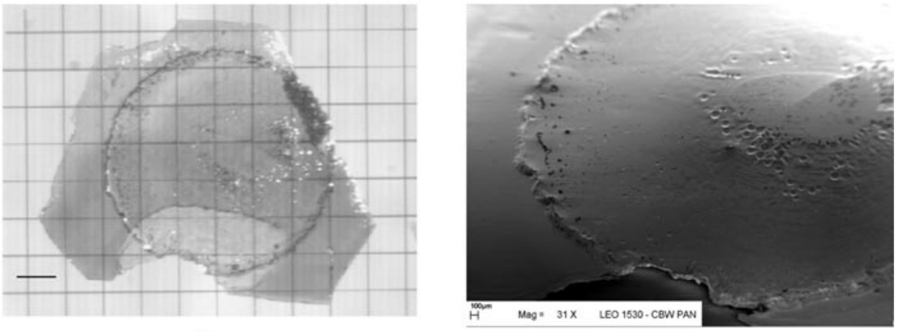

(a) (b)

Figure 11. GaN substrate with the new grown material on the Ga-polar surface: (a) optical image (distance between the grid lines, 1 mm), (b) SEM image.

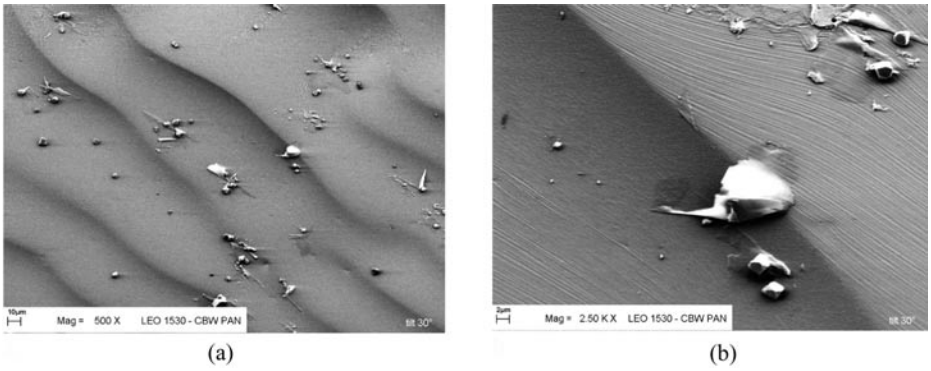

(a) (b)

Figure 12. Morphology of GaN crystal grown on Ga-polar surface of GaN substrate in a 50 h process. SEM images of the growth hillock surface in different magnifications.

The new material was transparent, colourless and grown as a single hillock 6 mm in diameter. The periodic, cellular structures were no longer present. The dominant growth mechanism was the propagation of the macrosteps from the hillock centre. The position of the hillock centre most probably corresponds to the minimum supersaturation being the result of the radial temperature gradients in the growth solution. The macrosteps are shown clearly in figures 12(a) and (b). Such growth features are often observed for crystallization from solutions since the surface diffusion is strongly limited in comparison to the growth from the vapour phase where the growth proceeds by the propagation of monoatomic steps.

The mechanism of the growth on the N-polar surface was also the propagation of the macrosteps; however the presence of several growth centres has been observed for the similar conditions of the experiment. It is still not clear if this is related to differences in nucleation mechanisms on the surface of different polarity or to the imperfect preparation of the surface which, in contrast to the Ga-polar one, is chemically active.

The normal growth rates observed in these experiments were 4–8 μm h^{-1} for both polarities, depending on supersaturation at the growth front being a function of temperature gradient and the height of Ga over the substrate. The microscopic observation of the cross sections of the samples (figure 13) showed that the growth was stable in terms of continuity of the new grown material. The inclusions of the solvent and/or voids were not observed. The interfaces between substrates (80–100 μm thick) and the new grown crystals were not visible, indicating that the surface preparation and the wetting procedures before seeding were performed correctly. The XRD analysis shows that the material grown by the method just described is of similar structural quality than the substrate used. So this kind of directional crystallization experiment will be continued to find the optimum configuration for stable growth of bulk GaN in $\langle 0001\rangle$ directions. In particular, in order to limit the step bunching, the supersaturation across the growing surface should be more uniform. This can be achieved by the reduction of radial temperature gradients and/or by decreasing of the height of Ga over the substrate.

As already mentioned, at the conditions similar to the conditions used for the spontaneous growth of the platelets, the seeded growth into directions perpendicular to the *c*-axis should occur relatively fast and in a stable way, especially into directions $\langle 11-20\rangle$. The preliminary results of such experiments are shown below. The seed crystals were prepared by cutting the GaN platelets as shown in figure 14.

The next figure shows both the expected and the example of the real result of growth in a 40 h process. Since the lateral size of the resulting crystal is determined by the initial length of

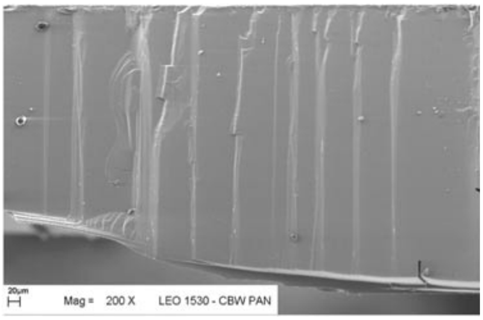

Figure 13. SEM scan of the cross section of GaN crystal grown on the Ga surface of the GaN substrate for 40 h.

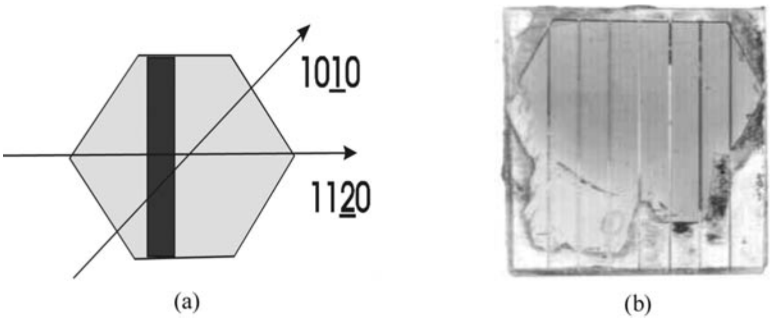

(a) (b)

Figure 14. Preparation of the seed crystal for the growth in the fastest growth ⟨11 − 20⟩ directions: (a) schematic view, (b) GaN platelet after cutting by the wire saw—the width of each seed is 1 mm.

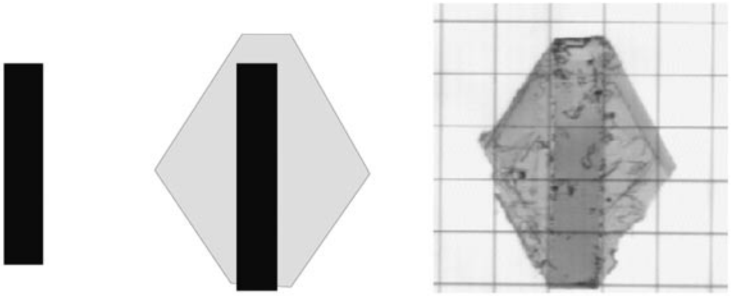

(a) (b) (c)

Figure 15. Seeded growth of GaN into ⟨11 − 20⟩ directions: (a) schematic view of the seed, (b) expected result of the growth, (c) result of the 40 h growth.

the seed, the method seems to be promising for the growth of GaN single crystalline platelets in a more reproducible way regarding their shape and distribution in the crucible.

6. Physical properties of GaN grown by HNPS method

6.1. Point defects

As already mentioned, the N_2 molecules dissociate at the contact with the Ga surface. However to approach the surface they have to overcome quite high (about 3.5 eV) potential barrier, which lowers substantially the rate of nitrogen dissociation and its further dissolution in the metal. For oxygen interacting with Ga, there is no potential barrier for dissociation [28] and therefore even traces of this impurity in the growth system are a source of unintentional oxygen doping of GaN. Consequently the crystals are strongly n type with free electron concentration of about 5×10^{19} cm^{-3} (metallic conductivity) and mobility of about 60 cm^2 V^{-1} s^{-1} [29]. These free carriers can be fully eliminated by Mg acceptor added to the growth solution. Then the resistivity of the crystals becomes as high as 10^4–10^6 Ω cm at 300 K. Usually the GaN:Mg crystals become p type with an activation energy of 150 meV, at temperatures slightly exceeding 300 K. More detailed analysis of the electrical properties of pressure grown Mg doped GaN crystals can be found in [30].

The presence of the native point defects in the crystals has been checked by positron annihilation measurements [31]. High concentration of Ga vacancies V_{Ga} has been found in the conductive crystals in contrast to the Mg-doped samples where no Ga vacancies have been observed. This agreed with the theoretical prediction that the formation energy of V_{Ga} decreases with the increase of the Fermi level energy [23, 24] suggesting that in the creation of these defects thermodynamics plays a role. The difference in the PL spectra [32] of the conductive (strong yellow emission) and Mg-doped crystals (no yellow emission, blue Mg-related signal) supported that V_{Ga} is involved in yellow luminescence in GaN.

A quite different picture is observed for doping with beryllium [33]. The GaN:Be crystals are also highly resistive with the constant activation energy of 1.46 eV at temperatures up to at least 1000 K. But their PL spectra are dominated by a very strong yellow luminescence and the crystals contain a lot of gallium vacancies [33] like the highly conductive crystals grown without intentional doping. So it is very probable that these crystals are n type during high temperature growth and become semi-insulating only during cooling down. Such behaviour can be related to the two possible configurations of Be atoms in the GaN lattice (Be_{Ga}—acceptor—and Be_i—donor) and their redistribution as a function of temperature.

Some faces corresponding to the polar low index {0001} and {10 − 11} crystallographic planes in wurtzite structure, appearing in the pressure grown GaN crystals, are non-equivalent regarding their atomic structure. This reflects in the asymmetry of the physical properties of the platelike crystals grown without an intentional seeding.

In figure 16 there is an example of such an asymmetry. The figure shows that the material grown with N polarity differs in its PL properties from the material grown with the Ga polarity, which indicates that the point defects incorporate into the crystal in different ways. Additionally the spectra coming from the material grown on the {0001} N- or Ga-polar surfaces (seeded growth) are of similar character to the spectra from corresponding surfaces of the substrate. Since the platelets were polished before being used as seeds, the suggestion arises that the platelets themselves also demonstrate a polar character despite being grown mainly in the fastest growth $\langle 10-10 \rangle$ directions, which follows from their morphology. The strong support for this is the measurements of the free electron concentration distribution across the cleaved, as-grown GaN platelet by the micro-Raman scattering technique [34]. Figure 17 shows that the border line between materials of higher (N-side) and lower (Ga-side) electron concentration is situated inside the crystal dividing it into two parts. This suggests that the microscopic (in the atomic scale) processes responsible for the formation of both native and impurity-related point defects occur mainly on the {10 − 11} polar faces of growing GaN crystals independently of whether the growth is perpendicular or parallel to the *c*-axis.

Such an approach allows better understanding of another result of positron annihilation measurements [35] showing that the concentration of Ga vacancies is much higher at the Ga side than at the N side of the n-type GaN platelets. It seems surprising at first sight, since on the Ga-polar (0001) surface, the surface Ga atoms are bonded to the surface by three bonds

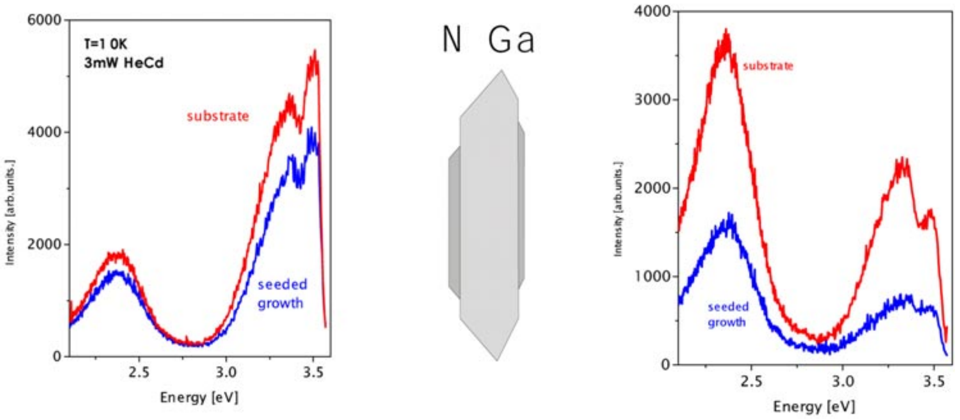

Figure 16. Photoluminescence of GaN grown on different sides of a polished platelet grown without intentional seeding (substrate) and the platelet (substrate) itself.

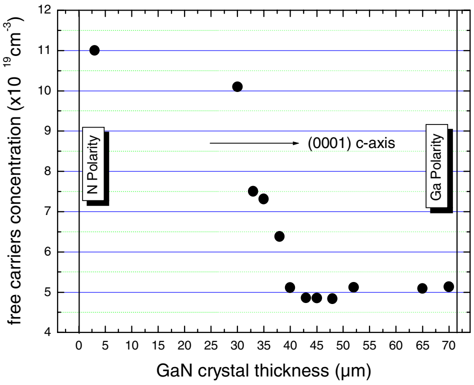

Figure 17. Distribution of free electron concentration across the GaN platelet measured by the micro-Raman scattering technique [34].

whereas to the opposite one only by one bond. If we assume however that the incorporation of the Ga atoms occurs on the $\{10-11\}$ polar surfaces, the positron annihilation results become more consistent since on the $(10-11)$ face adjacent to the (0001) one, the Ga atoms can be bonded by one or two bonds whereas on the opposite $(-101-1)$ polar surface adjacent to the $(000-1)$ one, the Ga surface atoms are bonded by two or three bonds. The arrangement of the atoms on the relevant polar surfaces of GaN is shown in figure 18. It follows from above that the lateral (perpendicular to the *c*-axis) growth of the platelet does not occur on the non-polar $\{10-10\}$ surfaces (at least it is not predominant) since then a plateau in the middle of the diagram of figure 17 should be observed.

6.2. *Extended defects*

The structure of the pressure grown GaN crystals has been studied by x-ray diffraction (XRD) [36], transmission electron microscopy (TEM) (i.e. [20, 37–39], defect selective etching (DSE) [39] and atomic force microscopy (AFM) of the homoepitaxial layers [40].

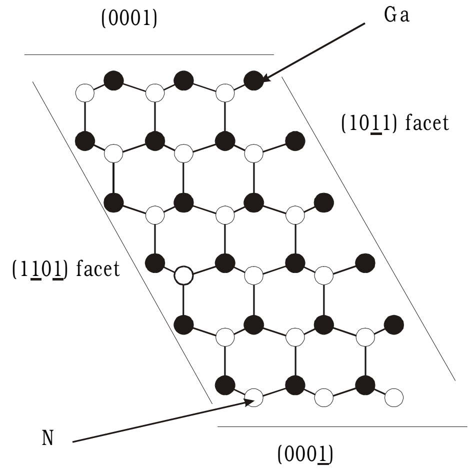

Figure 18. The arrangement of atoms on the polar surfaces of GaN.

For the conductive crystals, the shape of the x-ray rocking curves ((0002)Cu Kα reflection) depends on the size of the crystal. The full widths at half maximum (FWHMs) are 20–30 arcsec for 1 mm crystals and 30–40 arcsec for 1–3 mm ones. For larger platelets the rocking curves often split into a few $\sim$30–40 arcsec peaks showing a presence of low angle (1–3 arcmin) boundaries separating grains of a few mm in size. Misorientation between grains increases monotonically from end to end of the crystal [36]. It has been suggested that this may be also related to the polar character of the platelets growth leading to some strain and its subsequent relaxation through the formation of the low angle boundaries.

It was shown by Liliental–Weber *et al* [20], by TEM examination that the N-polar $(000-1)$ surface of the n-type pressure grown GaN crystals (especially for the smaller ones) is often atomically flat (2–3 monolayer steps present) and that the crystals under this surface are practically free of extended defects. Under the opposite, rough surface a number of extended defects like stacking faults, dislocation loops and Ga microprecipitates were observed. The relative thickness of this part usually consists of 10% of the entire thickness of the platelet. It seems that the presence of these defects is related to the growth instabilities often observed on the Ga-polar surface of the crystals grown without an intentional doping.

The detailed TEM studies of Mg-doped crystals are reported in [38]. In particular it is shown that the introduction of Mg induces the formation of set of specific extended defects, being mainly the stacking faults situated at the $\{0001\}$ polar surfaces of the investigated crystals.

For the use of the crystals as substrates for epitaxy, the near surface part of the material, being often the result of the unstable growth has to be removed by polishing and subsequent reactive ion etching (Ga-side) or mechano-chemical polishing (N-side) procedures. As a rule the extended defects are not observed by TEM in the crystals used as substrates for both N and Ga polarity epitaxial growth. Therefore, if the epitaxy is properly performed both the substrate and the layer quantum structure do not contain dislocations. Figure 19 shows two examples of the TEM scans of dislocation free multilayer structures grown on pressure grown GaN substrates of both polarities.

Unfortunately, the TEM technique allows us to analyse only very small area samples. Therefore in order to measure dislocation densities in GaN, the defect selective etching methods have been developed [39]. It was shown that etching in molten KOH–NaOH eutectics

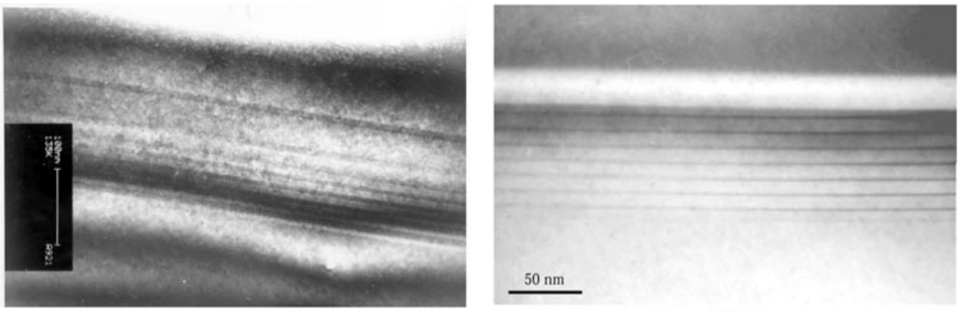

(a) (b)

Figure 19. TEM cross sections [37] of (a) a GaN/$Al_{0.1}Ga_{0.9}N$ multilayer structure grown by PA MBE on the N-polar surface of GaN substrate [42] and (b) a GaN/InGaN/AlGaN multilayer structure grown by MOCVD [41] on the Ga-polar surface of GaN substrate. No extended defects are observed in either the substrates or the layer structures.

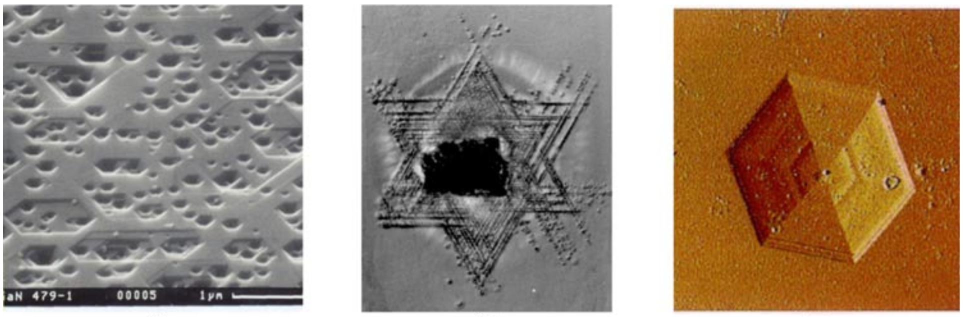

(a) (b) (c)

Figure 20. Defect selective etching of GaN: (a) a GaN/sapphire heteroepitaxial layer after etching in molten KOH–NaOH eutectics [39]; (b) a GaN pressure grown single crystal after indentation with diamond and etching in molten KOH–NaOH eutectics [39] (the average size of the star like pattern is 100 μm); (c) an etch pit (EP) on the GaN crystal surface after etching in molten KOH–NaOH eutectics [39], observed density of EPs 10–10^2 cm^2.

reveals dislocations in both GaN heteroepitaxial layers and GaN pressure grown single crystals. Examples are presented in figure 20. Figure 20(a) shows the result of defect selective etching of a typical GaN heteroepitaxial layer grown by MOCVD on sapphire substrate. The high density of the etch pits is clearly visible. The same method applied for bulk crystals gives a very small (10–100 cm^{-2}) number of the etch pits. A typical pit observed on both heteroepitaxial layers and crystals is shown in figure 20(c). The pattern in figure 20(b) is the result of DSE of a GaN single crystal with dislocations generated intentionally by indentation with diamond. The etch pits surround the imprint of the diamond, showing the area where dislocations are present and that the remaining material is dislocation free.

7. Concluding remarks

Despite the quite extreme pressures and temperatures required for crystallization of GaN from solutions of atomic N in liquid Ga, the crystal growth process is governed by the same rules as most well known solution growth processes. Therefore the control of GaN crystal growth can be still improved by the proper choice of the configuration and the conditions of the experiment.

The growth of GaN without intentional seeding results in dislocation free crystals in the form of thin hexagonal platelets reaching lateral dimensions of about 1 cm. Further scaling of the size of such crystals is possible as follows from the analysis of the crystallization process as a function of the growth time and the volume of the solution. The crystals can be used as substrates for epitaxial growth of dislocation free structures by both MBE and MOCVD methods. The properties of such structures were reviewed in [42].

The most important problems in obtaining bulk GaN well developed in ⟨0001⟩ directions are the small nucleation rates on the {0001} surfaces at low supersaturations and growth instabilities on these surfaces at higher supersaturations. To avoid the morphological instabilities, the supersaturation at the growing crystal faces has to be uniform and, to avoid the constitutional supercooling, it has to achieve its maximum at the crystallization front.

A significant improvement of the results of the growth in directions ⟨0001⟩, in terms of the growth rates and the morphological stability, was observed in vertically arranged directional crystallization on single crystalline GaN substrates. Further increase of the growth rates should be possible [26] by e.g. the application of a temperature gradient travelling solvent configuration. This technique gives the highest rates of stable crystallization from solutions since it allows the best control of supersaturation at the growing surface.

References

[1] Nakamura S and Fasol G 1997 *The Blue Laser Diodes* (Berlin: Springer)

[2] Amano H, Kito M, Hiramatsu K and Akasaki I 1989 *Japan. J. Appl. Phys.* **28** L139

[3] Nakamura S 2000 *IECE Trans. Electron.* **E83-C** 529

[4] Hiramatsu K and Usui A 1999 *EMIS Datareview Series 23* (London: INSPEC, The Institution of Electrical Engineers) p 440

[5] Amano H, Iwaya M, Hayashi N, Kashima T, Katsuragawa M, Takeuchi T, Wetzel C and Akasaki I 1999 *GaN and Related Alloys. Mater. Res. Soc. Symp. Proc.* (Warrendale, PA: Materials Research Society) pp G10.1.1/8

[6] Nishino K and Sakai S 1999 *EMIS Datareview Series* 23 (London: INSPEC, The Institution of Electrical Engineers) p 367

[7] Sukhoveyev V, Ivantsov V, Zubrilov A, Nikolaev V, Nikitina I, Bougrov V, Tsvetkov D and Dmitriev V 1998 *Mater. Sci. Forum* vol 264–8, pp 1331–4

[8] Inoue T, Seki Y, Oda O, Kurai S, Yamada Y and Taguchi T 2000 *Japan. J. Appl. Phys.* **39** 2394

[9] Schowalter L J, Rojo J C, Slack G A, Shusterman Y, Wang R, Bhat I and Arunmozhi G 2000 *J. Cryst. Growth* **211** 78

[10] Van Vechten J A 1973 *Phys. Rev.* B **7** 1479

[11] Karpinski J, Jun J and Porowski S 1984 *J. Cryst. Growth* **66** 1

[12] Karpinski J and Porowski S 1984 *J. Cryst. Growth* **66** 11

[13] Grzegory I 1995 Warunki krystalizacji zwiazkow A^{III}N w wysokim cisnieniu azotu *PhD Thesis* Warszawa

[14] MacChesney J B, Bridenbaugh P M and O'Connor P B 1970 *Mater. Res. Bull.* **5** 783

[15] Thurmond C D and Logan R A 1972 *J. Electrochem. Soc.* **119** 622

[16] Madar R, Jacob G, Hallais J and Fruchard R 1975 *J. Cryst. Growth* **31** 197

[17] Krukowski S, Romanowski Z, Grzegory I and Porowski S 1999 *J. Cryst. Growth* **189/190** 159

[18] Porowski S and Jun J 1994 unpublished

[19] Lucznik B, Adamczyk J, Jun J, Krukowski S and Grzegory I 1994 unpublished

[20] Liliental-Weber Z 1999 *EMIS Datareview Series 23* (London: INSPEC, The Institution of Electrical Engineers) p 230

[21] Rouviere J L, Weyher J L, Seelmann-Eggebert M and Porowski S 1998 *Appl. Phys. Lett.* **73** 668–70

[22] Seelmann-Eggebert M, Weyher J L, Obloh H, Zimmermann H, Rar A and Porowski S 1997 *Appl. Phys. Lett.* **71** 2635

[23] Neugebauer J and Van de Walle C G 1994 *Phys. Rev.* B **50** 8067

[24] Boguslawski P, Briggs E L and Bernholc J 1995 *Phys. Rev.* B **51** 17 255

[25] Tiller W A, Jackson K A, Rutter J W and Chalmers B 1953 *Acta Metall.* **1** 428

[26] Tiller W A 1968 *J. Cryst. Growth* **2** 345

[27] Weyher J L, Müller S, Grzegory I and Porowski S 1997 *J. Cryst. Growth* **182** 17

[28] Krukowski S, Bockowski M, Lucznik B, Grzegory I, Porowski S, Suski T and Romanowski Z 2001 *J. Phys.: Condens. Matter* **13** 1

[29] Perlin P, Camassel J, Knap W, Talercio T, Chervin J C, Suski T, Grzegory I and Porowski S 1995 *Appl. Phys. Lett.* **67** 2524

[30] Litwin-Staszewska E *et al* 2001 *J. Appl. Phys.* **12** 7960

[31] Saarinen K *et al* 1997 *Phys. Rev. Lett.* **79** 3030

[32] Porowski S *et al* 1997 *Acta Phys. Pol.* A **92** 958

[33] Suski T, Litwin-Staszewska E, Perlin P, Wisniewski P, Teisseyre H, Grzegory I, Bockowski M, Porowski S, Saarinen K and Nissila J 2000 *EGW-4 (Nottingham, 2000)*

[34] Frayssinet E 2000 Elaboration et etude d'heterojonctions GaN/AlGaN deposees sur GaN massif *PhD Thesis* Universite Montpellier II

[35] Suski T *et al* 1998 *Mater. Sci. Eng.* B **59** 1

[36] Leszczynski M, Grzegory I, Teisseyre H, Suski T, Bockowski M, Jun J, Baranowski J M, Porowski S and Domagala J 1996 *J. Cryst. Growth* **169** 235–42

[37] Christiansen S H, Albrecht M, Strunk H P, Foxon C T, Korakakis D, Grzegory I and Porowski S 1999 *Proc. ICNS'99 (Montpellier) Phys. Status Solidi* a **176** 285

[38] Liliental-Weber Z, Benamara M, Swider W, Washburn J, Grzegory I, Porowski S, Dupuis R D and Eiting C J 1999 *Physica* B **273/274** 124

[39] Weyher J L, Brown P D, Rouviere J L, Wosinski T, Zauner A R A and Grzegory I 2000 *J. Cryst. Growth* **210** 151

[40] Leszczynski M, Prystawko P and Nowak G 2000 private communication

[41] Leszczynski M and Prystawko P 2000 private communication

[42] Grzegory I 2001 *E-MRS Meeting (Strasbourg, 2000) Mater. Sci. Eng.* B **1–3** 30